

Use of CRISTA mesopause region temperatures for the intercalibration of ground-based instruments

J. Scheer^{a,*}, E.R. Reisin^a, O.A. Gusev^b, W.J.R. French^c, G. Hernandez^d, R. Huppi^e, P. Ammosov^f, G.A. Gavril'yeva^f, D. Offermann^b

^a Instituto de Astronomía y Física del Espacio, CONICET-UBA, Buenos Aires, Argentina

^b Physics Department, University of Wuppertal, Wuppertal, Germany

^c Space and Atmospheric Sciences, Australian Antarctic Division, Kingston, Tasmania, Australia

^d Department of Earth and Space Sciences, University of Washington, Seattle, WA 98195-1310, USA

^e Electrical and Computer Engineering, Utah State University, 6 Fairlane Terrace, Winchester MA 01890, USA

^f Institute of Cosmophysical Research and Aeronomy, Yakutsk, Russia

* Corresponding author: Instituto de Astronomía y Física del Espacio, Ciudad Universitaria, CC67-Suc. 28, 1428 Buenos Aires, Argentina. Fax: +54-11-4786-8114. Email address: jurgen@caerce.edu.ar

Abstract

Most available ground-based techniques for measuring temperatures in the upper mesosphere to lower thermosphere (or mesopause region) have systematic errors that are comparable to those of orbiting instruments. Determining these unknown biases would normally require colocated observations that are only seldom feasible. Satellite measurements can be used as a "transfer standard" between ground-based observations that are not colocated. In this context, even with a reproducible or known bias in the satellite data, the comparison is still meaningful. Since CRISTA temperatures cover the mesopause region with very good accuracy (statistical errors do not exceed 1.5 K and systematic uncertainties range from about 3 to 7.5 K), they are quite suitable for this purpose. Because of the nearly constant precision over the height range of interest, also rotational temperatures of airglow emissions from different altitudes like the OH and O₂ bands (or the OI558 nm line) can be successfully compared with each other. In spite of the limited number of overpasses during the relatively short CRISTA missions, the feasibility of such an intercalibration is demonstrated for widely separated ground-based sites. Here, the results obtained for ground-based measurements at eight different sites, using CRISTA-1 and CRISTA-2 data, are presented. For OH temperatures, the standard deviation between the different instruments is only 5.4 K, confirming previous estimates.

Keywords: Mesopause region, Temperature, Airglow, Satellite

1. Introduction

In the validation of satellite data by comparison against ground-based (GB) observations, the primary aim is establishing the quality of the satellite measurements. In such a case, the data against which the comparison is made should be more reliable than the instrument to be validated.

However, most available GB techniques for measuring temperatures in the upper mesosphere to lower thermosphere (or mesopause region, between about 80 and 100 km) have systematic errors comparable to those of orbiting instruments, or even greater.

The opposite approach, namely to use the satellite instrument as a "transfer standard" for an intercomparison of different GB instruments may also be useful, because it leads to the comparability of different measuring techniques obviating the need to transport them to the same site.

The idea has been pursued in the past (Torr et al., 1977), for the intercomparison of GB airglow photometers via the AE-C satellite. The target of that work was photometry and revealed considerable differences in the sensitivities of the GB photometers, pointing to problems with GB calibration procedures.

For upper atmospheric temperature measurements until about 65 km altitude, the intercalibration between the LIMS instrument on the Nimbus-7 satellite and meteorological rockets (Gille et al., 1984) has been one of the first applications of this technique. This led to an extensive intercomparison between US and USSR rocketsondes of the types that had been launched together only in two previous dedicated campaigns.

For mesopause region temperatures, a recent example is the paper by von Savigny et al. (2004), where satellite and GB rotational temperatures from OH airglow bands were compared, using the SCIAMACHY instrument on Envisat. Although mainly meant as a validation of the satellite instrument, it can also be considered as an example of an intercomparison between GB instruments at three different sites.

The quality of the recently refined retrieval of mesopause region temperatures from the Cryogenic Infrared Spectrometers and Telescopes for the Atmosphere (CRISTA) satellite instrument is so good that they can serve excellently as a transfer standard for GB instrument comparisons (see Gusev et al., this issue). The purpose of the present paper is to take advantage of this, the nearly global coverage of the two CRISTA missions, and the availability of GB observations at many sites, during the related campaigns.

2. Data available

Although the number of ground stations that took temperature measurements during the two CRISTA flights has been considerable (nearly two dozens), only about one third of these could be used in the present study because of the miss time and distance criteria that require nearly simultaneous CRISTA and GB observations, within a reasonable maximum distance (here, a radius of 1000 km was somewhat arbitrarily chosen). In principle, mesopause region temperatures from any source are suitable for this study. However, only temperatures derived from nocturnal airglow observations could actually be employed here, for meeting the criteria mentioned. Most of the available data are rotational temperatures of OH emissions in different Meinel bands (or as Doppler temperatures, from one site) that originate in a layer centered at 87 km, and 6-10 km wide. There are also rotational temperatures from the $O_2b(0-1)$ Atmospheric band, or Doppler temperatures of the OI558 nm emission line, available from two instruments. These emissions correspond to nominal heights of 95 or 96 km, respectively (with layer thickness not much different from OH).

Table 1 contains information about the instrumentation and data characteristics at the sites: Maimaga Observatory near Yakutsk (YAK) in Siberia; Booth Bay (BOO), Millstone Hill (MIH), and Wallops Island (WAL) in the United States; El Leoncito (LEO) and Buenos Aires (BUE) in Argentina; Mount John Observatory (MJO) in New Zealand; and Davis (DAV) in Antarctica. The geographical locations are given with respect to the field of view, at the altitude of the airglow layers. Also, references are given about theoretical transition probabilities and about descriptions of instrumentation and data reduction technique used, in each case. The different airglow bands and transition probabilities are expected to lead to different unrelated systematic errors in the determination of rotational temperatures (Turnbull and Lowe, 1989), which makes empirical

intercomparisons more necessary. The MJO data are Doppler temperatures that are expected to be free from such errors.

The CRISTA instrument and mission characteristics of the two flights in November 1994 and in August 1997 have been described by Offermann et al. (1999) and by Grossmann et al. (2002, 2004). CRISTA temperatures for the mesopause region are derived from limb radiance measurements of the CO₂ bands at 4.3 and 15 μm . A detailed description of the instrument characteristics, orbital geometry and other factors related to the temperature measurements during the CRISTA-1 mission has been given by Riese et al. (1999). An account of the determination of CO₂ densities necessary for temperature retrieval is contained in the paper by Kaufmann et al. (2002). The present data are based on the refined non-LTE temperature retrieval developed recently by Gusev et al. (this issue). It is important to understand that the vertical temperature profiles needed for the comparison with ground-based observations are obtained after a complex geometrical transformation from radiances integrated along an approximately horizontal path around the tangent point (for a given altitude) that involves horizontal averaging. This somewhat reduces the relevance of zero miss distance comparisons. Although the total time of measurements was 9 days during each flight, less than one half of the time was employed to determine mesopause region data. The fraction of time corresponding to nocturnal overpasses depends on latitude. During CRISTA-2, most northern latitudes only had daytime overpasses (Grossmann et al., 2002), making direct comparison with nighttime airglow observation impossible.

3. Processing

The CRISTA data from both missions were accessed through the CRISTA data management and visualization program GLOBAL that allows us to selectively extract the pertinent temperature data for the overpasses at the different geographical locations. Without this and other software tools, even the detection of overpass conditions would have been a laborious and error-prone task.

Individual CRISTA profiles during a single overpass can vary considerably. An example for an overpass at a midlatitude site (LEO) can be seen in Fig. 1 (left panel). The geometry of this overpass can be appreciated in the map view inserted in the right-hand panel, which presents the geographic position of the four tangent points relative to the LEO site, during the northward passage of CRISTA-2, on 14 August 1997 at about 9:10 UT. In spite of the small temporal spacing of the individual profiles that are not more than one minute apart, temperature differences reach 40 K, at some altitudes. This variation is almost completely geophysical, since the statistical error bars (not shown) do not exceed ± 1 K, at 87 km, and ± 1.5 K, at 100 km (Gusev et al., this issue). The vertical oscillations visible in the profiles are part of the 3-dimensional wave structure that also causes the difference between profiles. This complex wave structure, which CRISTA samples along its track, is a superposition of different modes of planetary waves (Ward et al., 2000; Smith et al., 2002) and tides (Ward et al., 1999; Oberheide and Gusev, 2002; Oberheide et al., 2000; 2003), including transients, and also some gravity waves (Preusse et al., 2001).

To improve the comparison with airglow-derived temperatures, CRISTA profiles are smoothed with a Gaussian weighting function of 8 km full width at half maximum, as an approximation to a typical vertical emission profile, for any of the three airglow emissions considered here. These filtered profiles are shown in the center panel of Fig. 1. The smoothing also reduces somewhat the variation from profile to profile. For the nominal altitudes of the airglow layers, at 87 and 95 km (or 96 km, for the OI558 emission), "airglow-equivalent" CRISTA temperatures T_c are thus defined, and are used instead of the values taken from the raw profiles, in the following analysis. Although variations from the nominal airglow emission altitudes by a few kilometers are known to occur, we assume, as is usually done in airglow work, that the nominal values are good approximations and do not introduce serious errors, on average. The estimates of the possible error due to this altitude

uncertainty that we give for examples from LEO and MJO (see below) show that this assumption is reasonable.

Fig. 2 gives an impression of the typical relation between temporal variations of CRISTA and GB temperatures during the same overpass. The figure shows a one-hour section of the data from LEO centered on the CRISTA passage. The upper panel compares O₂ temperatures to airglow-equivalent CRISTA data for 95 km, while the lower panel does the same for OH and CRISTA temperatures at 87 km. Error bars for the airglow data are derived from photon counting statistics for each point (Reisin and Scheer, 2004). Since the statistical errors for CRISTA are only slightly greater than the size of the symbols, they are omitted here.

The scatter of the CRISTA temperatures is greater than that of the airglow data. This reflects the fact that the spatial variation (due to medium- and large-scale waves, as mentioned) sampled by CRISTA surpasses the short-term temporal variability at a fixed ground station. Ground station variability cannot be so strong. For instance, at a fixed place, the tidal variation corresponding to the greatest observed semidiurnal amplitudes of 25 K does not exceed 0.2 K/min, and a strong gravity wave with 10 min period and 5 K amplitude creates a maximum variation of only about 3 K/min. On the other hand, during the overpass in Fig. 2, CRISTA temperatures at 95 km vary by 20 K in less than a minute, during which the satellite moves by about 400 km. At 87 km, neighbouring CRISTA points vary by as much as 16 K, over the same time span and distance. There is however no prominent correlation between the CRISTA and LEO data, at the timescale of an overpass.

Two different overpasses at DAV (incidentally for the same date as Fig. 2) are documented in Fig. 3, with OH temperatures and CRISTA observations at 87 km. The upper panel focusses on the 17:55 UT overpass, and the lower one on the following overpass near 19:30 UT. In the latter case, the six CRISTA profiles involved are the maximum number possible within the 1000 km miss distance circle under normal (non "stare mode") observing conditions. Geophysical variability as sampled by CRISTA appears only small, here. However, this is not the typical situation at DAV, where CRISTA sees even stronger variations than at LEO, in most overpasses. Namely, the mean standard deviation within the individual overpasses at DAV (including those without GB data) was 8.9 K, while at LEO, it was 6.5 K. So, both figures give an idea of how strongly the observed variability can actually differ.

Since there is no simple regularity in the variation of CRISTA temperatures with miss distance, there is no straightforward way to extrapolate to zero miss distance, and so get rid of the bias from the spatial modulation. This would require a more detailed knowledge of the 3-dimensional spatial structure of the wave system than available from the limited sampling resolution. Therefore, we can only compare directly with the simultaneous GB data, without taking distances into account (except for the 1000 km miss distance limit), hoping that statistics will help to reduce bias. Of course, such a hope could only be more fully justified for missions of long duration, when a considerable number of overpasses is available at each site. For the short-duration CRISTA flights, this neglect of miss distance may affect some of our results.

Instead of individual GB temperatures (T_g), it is preferable to use averages $\langle T_g \rangle_j$ over intervals around each overpass sufficiently long to reduce the noise level below that due to the spatial variations. For the data at several sites, averaging over such "miss time intervals" (MTI) of ± 15 min was adequate, but for some instruments, longer intervals were chosen. For each overpass, the mean airglow-equivalent CRISTA temperature over the individual profiles is determined,

$$\langle T_c \rangle_j = \frac{1}{P_j} \sum_{i=1}^{P_j} T_{c_i}$$

where P_j is the number of profiles in overpass j , and the T_{c_i} are the airglow-equivalent CRISTA temperatures, as mentioned. For the LEO overpass example given above, this process leads to the

mean filtered profile in the right-hand panel of Fig. 1. The uncertainty in the true airglow emission height leads to an effect of only 1 to 2 K/km, in this example, which is expected to diminish with averaging over several overpasses.

$\langle T_c \rangle_j$ is then subtracted from the average GB temperature $\langle T_g \rangle_j$. The mean difference $\langle T_d \rangle$ is obtained for each site, weighted by the number of CRISTA profiles P_j ,

$$\langle T_d \rangle = \frac{\sum_{j=1}^N P_j (\langle T_g \rangle_j - \langle T_c \rangle_j)}{\sum_{j=1}^N P_j},$$

where N is the number of overpasses at the site.

The one-sigma uncertainty of $\langle T_d \rangle$ and the standard deviation (SD) are computed in a manner consistent with the weighting by the number of profiles. This implies that the number of statistical degrees of freedom (*dof*) is the total number of CRISTA profiles used. Although there should be no systematic bias due to random fluctuations, the quality of the statistical estimator of SD degrades inevitably for small *dof*.

In addition to this direct overpass ("zero" miss time) method, it would have been desirable to be able to process data for daytime overpasses using GB data from neighboring nights. This would have increased the number of overpasses and data available from other sites. However, tidal effects, especially from the diurnal tide, can be expected to defeat such a scheme. Comparison of daytime CRISTA data with the average of GB temperatures obtained in the previous and following nights indeed showed results appreciably different from those obtained by night overpasses alone. Because of the unpredictable day-to-day and day-to-night variability, these tidal effects cannot be corrected without additional information. Therefore, this alternative method had to be abandoned, and the analysis had to be based exclusively on direct overpass data.

4. Results and discussion

Table 2 lists the ground-based (GB) and CRISTA data corresponding to each of the direct overpasses, at the different sites (in the same alphabetic order as in Table 1). Data type is distinguished by the labels OH, O₂, or OI for the nominal altitudes 87, 95, and 96 km, respectively. Date, day of the year (doy), and overpass time are given consistently with respect to universal time. Miss time intervals used in the calculation of the mean GB data $\langle T_g \rangle$ are as listed in table 3. P is the number of CRISTA profiles with the mean temperature $\langle T_c \rangle$ at the nominal altitude, and $T_d = \langle T_g \rangle - \langle T_c \rangle$ is the corresponding temperature offset.

The mean results of the intercomparison for each site are shown in Table 3. The standard deviation describes the repeatability of an individual GB minus CRISTA comparison, with the main contribution due to spatial variability. The maximum miss time interval (MTI) has been increased from the default value of ± 15 min whenever necessary to ensure that the GB noise level stays below the uncertainty from the spatial variability.

The most reliable result in the table is obtained at DAV, due to the considerable number of overpasses and CRISTA-2 profiles. On average, OH temperatures at DAV are nearly 5 K higher than CRISTA temperatures at 87 km, with an uncertainty of only 1.4 K. Note that the DAV data are derived with Einstein coefficients after Langhoff et al. (1986), and that use of the improved empirical values by French et al. (2000) would reduce the offset to about 2.8 K. This result thus lends credibility to the empirical Einstein coefficients.

The results for LEO are based on nine CRISTA profiles during three overpasses. Because of this relatively good statistics, the conclusions about offsets different from zero can therefore be drawn

with confidence. While there is a negative bias of about 7 K, for OH temperatures, there is a positive one of nearly 16 K for O₂ temperatures. A very useful conclusion from these results, which has not been available otherwise, is the offset between the absolute scales of the OH and O₂ temperatures obtained with the Argentine airglow spectrometer. Although both parameters are measured with the same instrument, systematic errors for both emissions are independent, because of the different transition probabilities. The present results mean that for the data set obtained at LEO since August 1997, the O₂ temperatures had a bias of 22.3 ± 4.3 K with respect to the OH temperatures, so that it now becomes possible to talk about temperature differences between both altitudes in absolute terms, and to derive vertical temperature gradients from these data. Note that the uncertainty in this bias does not include a small effect of systematic errors from CRISTA (see Gusev et al., this issue). Since only the difference of these errors at the two altitudes matters, a contribution not greater than ± 1.5 K from this source should be expected.

There is a zero offset for the data at BOO, supported by five CRISTA-1 profiles in 4 overpasses. For MIH, the offset is only slightly positive (less than 3 K). Because of the small geographical separation between the fields of view of the instruments at MIH and BOO (350 km), all four CRISTA profiles corresponding to MIH coincide with those at BOO (see Table 2), and therefore the errors are not completely uncorrelated. The closeness between the results at both sites (within the combined error bars) is what one would expect of two instruments with the same characteristics and data reduction technique (Espy et al., 1995).

The result for WAL is derived from three CRISTA-1 profiles, each in a different overpass (two profiles are shared with MIH and BOO). The offset is nearly 4 K, but the error bar makes this still consistent with zero. Since this same instrument has been used at different sites, including during colocated comparisons of the other University of Wuppertal spectrometer, GRIPS-2 (Graef, 1991), this result has consequences beyond the operation at WAL (see also, von Savingy et al., 2004).

GB data for only one overpass in 1997 are available at MJO, and therefore results are more subject to statistical uncertainties than the previous cases. However, the data are particularly valuable for this comparison because they are Doppler temperatures, not rotational temperatures, and therefore do not depend on poorly known transition probabilities. Since there were four CRISTA profiles to compare with, the contribution of spatial variability to the final error can be estimated directly, while the GB contribution must be deduced from T_g statistics. OH Doppler temperature, with an offset of about -3 K, is well consistent with CRISTA. The Doppler temperature derived from the OI 558 nm line, with an emission layer nominally centered at 96 km, has a considerable positive bias of nearly 20 ± 6 K, contrary to expectation. Emission height changes even by several kilometers do not affect the outcome by more than 1 K, in this case. Such an offset, taken at face value, would be difficult to explain. However, the miss distance effect may have played an important role: during closest approach (192 km miss distance), the offset was only +8.9 K. That is, the main contribution to the mean offset comes from the data at greater miss distance (340 to 970 km). The offset may also be affected by the systematic error of CRISTA, estimated to be 6 K at this altitude. Thus, the discrepancy may be not as serious as it seems.

At YAK, the offset obtained is 1 ± 8 K, based on only one CRISTA-1 profile (as also occurred for BUE, see below). Since the error bar cannot be determined explicitly from the data alone, as in the cases with more than one overpass, the error is estimated from the variability of individual CRISTA profiles during a single overpass at LEO (6.5 K, as mentioned above). This value does not include variations between different overpasses, and is used as an ad-hoc estimator expected to be applicable everywhere, when there is no better alternative. Combined with the statistical error of $\langle T_g \rangle$ at YAK, the error given in parentheses in Table 3 is obtained. The good agreement is also interesting because little is known about the reliability of the transition probabilities used in this case (given by Krassovsky et al., 1962).

At BUE, with also only one CRISTA-1 profile to compare with, error analysis must be done in the same way as for YAK. Although the instrument is the same as that used at LEO, a different optical

filter was employed, and spectral background from strong city light contamination had to be corrected for, so that the data at BUE and LEO need not be expected to agree. For OH temperature, an offset of about 12 ± 8 K results, and for O₂, of about 7 ± 8 K. The behaviour for OH is really different in comparison with LEO, but for O₂ the offset is still similar, within the large error margin. The results for BUE are applicable only for the measuring conditions that prevailed during the 1994 campaign, because filter characteristics were probably also different from previous campaigns. The present results have no impact on the long-term trend analysis performed with this instrument (Reisin and Scheer, 2002), since the 1994 data were not used there.

An overview of the results can also be gleaned from Fig. 4, where the offsets between GB and CRISTA temperatures are plotted, for the eight different sites. The figure establishes the relation between data sets that were obtained with different techniques, at different times and widely separated locations. As mentioned, the error bars represent the effects of the observed fluctuations as obtained from the statistical analysis, as if they were quasi-random fluctuations, but the averages may still suffer some bias from poorly compensated statistics. The black dots correspond to rotational temperatures of four different OH bands and one set of OH Doppler temperature measurements. In spite of the different techniques, vibrational levels, or transition probabilities, the standard deviation is surprisingly low: only 5.4 K (but consistent with previous ad-hoc estimates of the systematic uncertainty due to instrumental and theoretical contributions, e.g., Scheer et al., 1994). Note especially that the figure suggests no noticeable dependence on the transition probabilities used for OH rotational temperatures (at DAV and YAK, coefficients other than those by Mies (1974) were employed).

The three points belonging to O₂ rotational and OI Doppler temperatures (open circles) show considerable positive offsets with respect to CRISTA. However, some part of the offsets might be attributable to the systematic uncertainty of CRISTA. The high positive bias for OI temperature at MJO may be, at least in part, due to a poor cancellation of the spatial variations sampled by CRISTA, as mentioned above.

5. Conclusions

Ground-based mesopause region temperature measurements corresponding to the altitude of OH airglow centered at 87 km at eight different, geographically remote sites have been compared to CRISTA data, during the CRISTA-1 mission in 1994 or the CRISTA-2 mission in 1997. The comparison is also made, at three sites, with temperatures derived from an O₂ band or the OI558 nm line. This establishes intercalibrations between different instruments at different sites and at different times. It also gives the offset between the absolute scales of OH and O₂ "thermometers", so that temperatures at 87 and 95 km in the data set from El Leoncito now become directly comparable.

The results obtained are not only relevant for comparisons between the data sets involved in this study, but may also be extended to equivalent data obtained at other times. Eventually, the results can be linked with other instruments that have directly or indirectly been intercompared, elsewhere, or will be, in the future.

Naturally, the precision of these results is limited by the short duration of the CRISTA flights, even in spite of the excellent quality of the CRISTA data. Long-duration satellite missions are needed to achieve smaller uncertainties in future intercomparisons of this kind, for a greater number of ground stations. The SABER instrument (Russell et al., 1999) on the TIMED satellite has the potential to play this role.

Acknowledgements

The authors wish to acknowledge the active participation of the many ground-based observers taking part in the two campaigns that accompanied the two CRISTA/MAHRSI missions, as well as

those colleagues who supplied data that could not be included here for not meeting the overpass conditions. Valuable help by M. Jarisch about the use of the CRISTA data base program GLOBAL is gratefully acknowledged. The CRISTA project is funded by grant 50 QV 9802-4 of the Bundesministerium für Bildung und Forschung (BMBF, Bonn, Germany) through Deutsches Zentrum für Luft- und Raumfahrt (DLR, Bonn). The first author thanks his hosts for the opportunity to work during one month as invited scientist at the University of Wuppertal. The observations from Mount John Observatory were supported by grant NSF-ATM-0109353. J.S. and E.R.R. acknowledge funding through ANPCyT grant PICT 12187.

References

- Ammosov, P.P., Gavriilyeva, G.A., Ignatyev, V.M., 1992. Registration of wave disturbances over Yakutia. *Advances in Space Research* 12(10), 145-150.
- Bittner, M., Offermann, D., Graef, H.-H., Donner, M., Hamilton, K., 2002. An 18-year time series of OH rotational temperatures and middle atmosphere decadal variations. *Journal of Atmospheric and Solar-Terrestrial Physics* 64(8-11), 1147-1166.
- Espy, P.J., Huppi, R., Manson, A., 1995. Large-scale, persistent latitude structures in the mesospheric temperature during ANLC-93. *Geophysical Research Letters* 22, 2801-2804.
- French, W.J.R., Burns, G.B., Finlayson, K., Greet, P.A., Lowe, R.P., Williams, P.F.B., 2000. Hydroxyl (6-2) airglow emission intensity ratios for rotational temperature determination. *Annales Geophysicae* 18, 1293-1303.
- Gille, J.C., Bailey, P.L., Beck, S.A., 1984. A comparison of U.S. and USSR rocketsondes using LIMS satellite temperature sounding as a transfer standard. *Journal of Geophysical Research* 89(D7), 11,711-11,715.
- Graef, H.-H., 1991. Bestimmung der Variabilität der Mesopausen-Temperatur aus OH* - Emissionen. *Sci. Rep. WU D-91-23*, University of Wuppertal, 42097 Wuppertal, Germany.
- Grossmann, K.U., Offermann, D., Gusev, O., Oberheide, J., Riese, M., Spang, R., 2002. The CRISTA-2 mission. *Journal of Geophysical Research* 107(D23), 8173, doi: 10.1029/2001JD000667.
- Grossmann, K.U., Gusev, O., Kaufmann, M., Kutepov, A., Knieling, P., 2004. A review of the scientific results from the CRISTA missions. *Advances in Space Research* 34(8), 1715-1721.
- Gusev, O., Kaufmann, M., Grossmann, K.U., Schmidlin, F.J., Shepherd, M.G., 2006. Atmospheric neutral temperature distribution at the mesopause altitude. *Journal of Atmospheric and Solar-Terrestrial Physics*, this issue, doi:10.1016/j.jastp.2005.12.010.
- Hernandez, G., Smith, R.W., Fraser, G.J., 1995. Antarctic high-latitude mesospheric dynamics. *Advances in Space Research* 16(5), 71-80.
- Kaufmann, M., Gusev, O.A., Grossmann, K.U., Roble, R.G., Hagan, M.E., Hartsough, C., Kutepov, A.A., 2002. The vertical and horizontal distribution of CO₂ densities in the upper mesosphere and lower thermosphere as measured by CRISTA. *Journal of Geophysical Research* 107(D23), 8182, doi:10.1029/2001JD000704.
- Krassovsky, V.I., Shefov, N.N., Yarin, V.I., 1962. Atlas of the airglow spectrum 3000 - 12400 Å. *Planetary and Space Science* 9, 883-915.

- Langhoff, S.R., Werner, H.-J., Rosmus, P., 1986. Theoretical transition probabilities for the OH Meinel system. *Journal of Molecular Spectroscopy* 118, 507-529.
- Mies, F.H., 1974. Calculated vibrational transition probabilities of OH($X^2\Pi$). *Journal of Molecular Spectroscopy* 53, 150-180.
- Oberheide, J., Gusev, O.A., 2002. Observation of migrating and nonmigrating diurnal tides in the equatorial lower thermosphere. *Geophysical Research Letters* 29, 2167, doi:10.1029/2002GL016213.
- Oberheide, J., Hagan, M., Ward, W.E., Riese, M., Offermann, D., 2000. Modeling the diurnal tide for the Cryogenic Infrared Spectrometers and Telescopes for the Atmosphere (CRISTA) 1 time period. *Journal of Geophysical Research* 105(A11), 24,917-24,929.
- Oberheide, J., Hagan, M.E., Roble, R.G., 2003. Tidal signatures and aliasing in temperature data from slowly precessing satellites. *Journal of Geophysical Research* 108(A2), 1055, doi:10.1029/20JA009585.
- Offermann, D., Grossmann, K.-U., Barthol, P., Knieling, P., Riese, M., Trant, R., 1999. Cryogenic Infrared Spectrometers and Telescopes for the Atmosphere (CRISTA) experiment and middle atmosphere variability. *Journal of Geophysical Research* 104, 16311-16325.
- Preusse, P., Eckermann, S.D., Oberheide, J., Hagan, M.E., Offermann, D., 2001. Modulation of gravity waves by tides as seen in CRISTA temperatures. *Advances in Space Research* 27(10), 1773-1778.
- Reisin, E.R., Scheer, J., 2002. Searching for trends in mesopause region airglow intensities and temperatures at El Leoncito. *Physics and Chemistry of the Earth* 27(6-8), 563-569.
- Reisin, E.R., Scheer, J., 2004. Gravity wave activity in the mesopause region from airglow measurements at El Leoncito. *Journal of Atmospheric and Solar-Terrestrial Physics* 66(6-9), 655-661.
- Riese, M., Spang, R., Preusse, P., Ern, M., Jarisch, M., Offermann, D., Grossmann, K.-U., 1999. Cryogenic Infrared Spectrometers and Telescopes for the Atmosphere (CRISTA) data processing and atmospheric temperature and trace gas retrieval. *Journal of Geophysical Research* 104, 16349-16367.
- Russell, J.M. III, Mlynczak, M.G., Gordley, L.L., Tansock, J., Esplin, R., 1999. An overview of the SABER experiment and preliminary calibration results. 44th Annual SPIE Meeting, July 18-23, Denver, Colorado, *Proceedings of the SPIE* 3756, 277-288.
- Scheer, J., Reisin, E.R., 2001. Refinements of a classical technique of airglow spectroscopy. *Advances in Space Research* 27(6-7), 1153-1158.
- Scheer, J., Reisin, E.R., Espy, J.P., Bittner, M., Graef, H.H., Offermann, D., Ammosov, P.P., Ignatyev, V.M., 1994. Large-scale structures in hydroxyl rotational temperatures during DYANA. *Journal of Atmospheric and Terrestrial Physics* 56, 1701-1715.
- Smith, A.K., Preusse, P., Oberheide, J., 2002. Middle atmosphere Kelvin waves observed in Cryogenic Infrared Spectrometers and Telescopes for the Atmosphere (CRISTA) 1 and 2 temperature and trace species. *Journal of Geophysical Research* 107(D23), 8177, doi: 10.1029/2001JD000577.
- Torr, M.R., Hays, P.P., Kennedy, B.C., Walker, J.C.G., 1977. Intercalibration of airglow observatories with the Atmosphere Explorer satellite. *Planetary and Space Science* 25(2), 173-184.

Turnbull, D.N., Lowe, R.P., 1989. New hydroxyl transition probabilities and their importance in airglow studies. *Planetary and Space Science* 37, 723-738.

von Savigny, C., Eichmann, K.-U., Llewellyn, E.J., Bovensmann, H., Burrows, J.P., Bittner, M., Höppner, K., Offermann, D., Taylor, M.J., Zhao, Y., Steinbrecht, W., Winkler, P., 2004. First near-global retrievals of OH rotational temperatures from satellite-based Meinel band emission measurements. *Geophysical Research Letters* 31, L15111, doi:10.1029/2004GL020410.

Ward, W.E., Oberheide, J., Riese, M., Preusse, P., Offermann, D., 1999. Tidal signatures in temperature data from CRISTA 1 mission. *Journal of Geophysical Research* 104, 16391-16403.

Ward, W.E., Oberheide, J., Riese, M., Preusse, P., Offermann, D., 2000. Planetary wave two signatures in CRISTA 2 ozone and temperature data. *Geophysical Monograph* 123, 319-325.

Watson, J.K.G., 1968. Rotational line intensities in $^3\Sigma\text{-}^1\Sigma$ electronic transitions. *Canadian Journal of Physics* 46(14), 1637-1643.

Table 1

Observation sites and ground-based instrumentation. (Stc=station code; IF=interferometer; SP=spectrometer)

Stc	Obs. site	Geogr. loc. (fov)		Airglow emission	Theor. coeff.	Instrument type	Instrument reference
BOO	Booth Bay	44.67°N	69.68°W	OH(3-1), (4-2)	Mies 1974	Michelson IF	Espy et al. 1995
BUE	Buenos Aires	34.59°S	58.44°W	OH(6-2), O2(0-1)	Mies 1974, Watson 1968	Tilting filter SP	Scheer & Reisin 2001
DAV	Davis	68.58°S	77.97°E	OH(6-2)	Langhoff et al. 1986	Czerny-Turner SP	French et al. 2000
LEO	El Leoncito	31.80°S	69.30°W	OH(6-2), O2(0-1)	Mies 1974, Watson 1968	Tilting filter SP	Scheer & Reisin 2001
MIH	Millstone Hill	41.83°N	71.50°W	OH(3-1), (4-2)	Mies 1974	Michelson IF	Espy et al. 1995
MJO	Mt. John	43.98°S	170.42°E	OI558, OH	Doppler	Fabry-Perot IF	Hernandez et al. 1995
WAL	Wallops Island	37.93°N	75.47°W	OH(3-1)	Mies 1974	Ebert-Fastie SP	Bittner et al. 2002
YAK	Yakutsk	63 °N	129.5 °E	OH(7-3)	Krassovsky et al. 1962	Grating SP	Amosov et al. 1992

Table 2

Ground-based ($\langle T_g \rangle$) and CRISTA data ($\langle T_c \rangle$) for each overpass at sites Stc. Data type DT distinguishes airglow emission and corresponding CRISTA altitude. $T_d = \langle T_g \rangle - \langle T_c \rangle$, and P gives the number of CRISTA profiles. Times and dates are in UT.

Stc	DT	date	day	$\langle T_g \rangle$	overpass time	P	$\langle T_c \rangle$	T_d
BOO	OH	94/11/04	308	211.73 ± 2.03	23:42:35	1	203.07	8.66
BOO	OH	94/11/05	309	204.80 ± 1.61	01:14:22	1	209.19	-4.39
BOO	OH	94/11/08	312	207.20 ± 1.99	22:41:59	1	208.54	-1.34
BOO	OH	94/11/09	313	198.83 ± 4.77	22:48:28 - 22:52:00	2	199.77 ± 0.36	-0.93
BUE	O2	94/11/10	314	209.64 ± 4.47	02:16:45	1	202.80	6.84
BUE	OH	94/11/10	314	196.33 ± 4.77	"	1	184.82	11.51
DAV	OH	97/08/13	225	200.50 ± 2.26	14:44:23 - 14:45:53	2	203.00 ± 2.72	-2.51
DAV	OH	97/08/13	225	203.29 ± 1.30	16:16:07 - 16:17:59	3	196.90 ± 2.97	6.38
DAV	OH	97/08/13	225	185.41 ± 6.23	17:47:20 - 17:50:36	3	192.37 ± 5.06	-6.96
DAV	OH	97/08/13	225	201.91 ± 1.41	19:19:57 - 19:24:12	5	197.61 ± 5.27	4.30
DAV	OH	97/08/13	225	191.27 ± 2.68	22:27:09	1	196.71	-5.44
DAV	OH	97/08/14	226	199.70 ± 6.20	14:49:39 - 14:50:38	2	193.57 ± 7.65	6.13
DAV	OH	97/08/14	226	194.77 ± 3.53	16:19:59 - 16:23:15	4	191.94 ± 3.33	2.83
DAV	OH	97/08/14	226	194.02 ± 5.05	17:52:36 - 17:56:51	5	183.93 ± 2.48	10.08
DAV	OH	97/08/14	226	198.69 ± 2.98	19:25:19 - 19:30:27	6	187.87 ± 0.92	10.82
DAV	OH	97/08/14	226	193.96 ± 3.71	20:58:02 - 21:00:48	4	188.81 ± 3.02	5.15
LEO	O2	97/08/13	225	206.50 ± 3.90	23:38:36 - 23:40:29	3	189.12 ± 3.33	17.38
LEO	OH	97/08/13	225	173.13 ± 2.46	"	3	187.54 ± 1.38	-14.41
LEO	O2	97/08/14	226	213.00 ± 1.12	09:07:41 - 09:10:26	4	194.30 ± 5.03	18.70
LEO	OH	97/08/14	226	193.38 ± 0.74	"	4	196.82 ± 6.06	-3.43
LEO	O2	97/08/15	227	195.14 ± 1.44	09:14:06 - 09:14:59	2	188.30 ± 4.22	6.83
LEO	OH	97/08/15	227	188.28 ± 1.02	"	2	189.93 ± 1.68	-1.64
MIH	OH	94/11/05	309	213.05 ± 1.50	01:14:22	1	209.19	3.86
MIH	OH	94/11/08	312	206.93 ± 2.73	22:41:59	1	208.54	-1.61
MIH	OH	94/11/09	313	204.23 ± 1.58	22:48:28 - 22:52:00	2	199.77 ± 0.36	4.47
MJO	OI	97/08/08	220	211 ± 4	09:39:05 - 09:42:20	4	191.17 ± 4.53	19.94
MJO	OH	97/08/08	220	184 ± 6	"	4	186.62 ± 1.84	-2.62
WAL	OH	94/11/05	309	205.28 ± 4.92	01:14:22	1	209.19	-3.92
WAL	OH	94/11/09	313	195.10 ± 3.04	00:17:19	1	184.23	10.87
WAL	OH	94/11/09	313	204.28 ± 1.76	22:52:00	1	200.13	4.15
YAK	OH	94/11/05	309	218.88 ± 4.53	10:10:59	1	217.87	1.01

Table 3

Comparison of GB rotational temperatures of OH (87km) and O₂/OI558 (95km/96km) with CRISTA overpass temperatures, at the different ground stations. Station codes (Stc) are as defined in Table 1. CRISTA missions 1 and 2 are distinguished in column CR. MTI is the (nominal) miss time interval used, $\langle T_d \rangle$ the mean difference between GB and CRISTA temperature (see text for details), accompanied by one-sigma error and standard deviation (SD), *dof* the number of CRISTA profiles, and *ovp* the number of overpasses. For *dof*=1, errors are estimated from typical standard deviations (in parentheses; see text).

Stc	CR	MTI [min]	$\langle T_d \rangle$ (87km) [K]	SD [K]	$\langle T_d \rangle$ (95km) [K]	SD [K]	<i>dof</i>	<i>ovp</i>
BOO	1	± 30	0.2 ± 2.2	4.9			5	4
BUE	1	± 15	11.5 ± (8.1)	(8.1)	6.8 ± (7.9)	(7.9)	1	1
DAV	2	± 15	4.8 ± 1.4	8.2			35	10
LEO	2	± 15	-6.7 ± 3.2	9.6	15.6 ± 2.9	8.7	9	3
MIH	1	± 40	2.8 ± 1.5	3.0			4	3
MJO	2	± 75	-2.6 ± 6.3	12.6	19.8 ± 6.0*	12.0	4	1
WAL	1	± 15	3.7 ± 4.3	7.4			3	3
YAK	1	± 75	1.0 ± (7.9)	(7.9)			1	1

* OI558nm Doppler temperature at 96 km

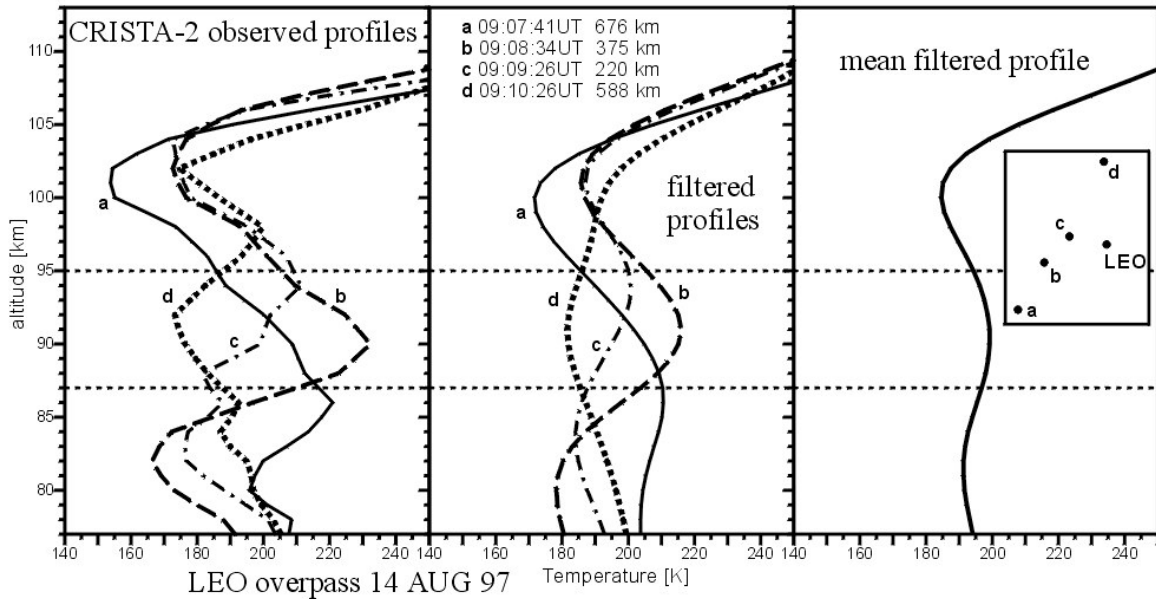


Fig. 1. Example of CRISTA profiles for one overpass at El Leoncito (LEO), for the overpass times and miss distances corresponding to the labels a-d, and the map view (right-hand insert). Center panel shows profiles weighted with airglow-equivalent Gaussian shape (see text). Horizontal dashed lines mark nominal airglow levels.

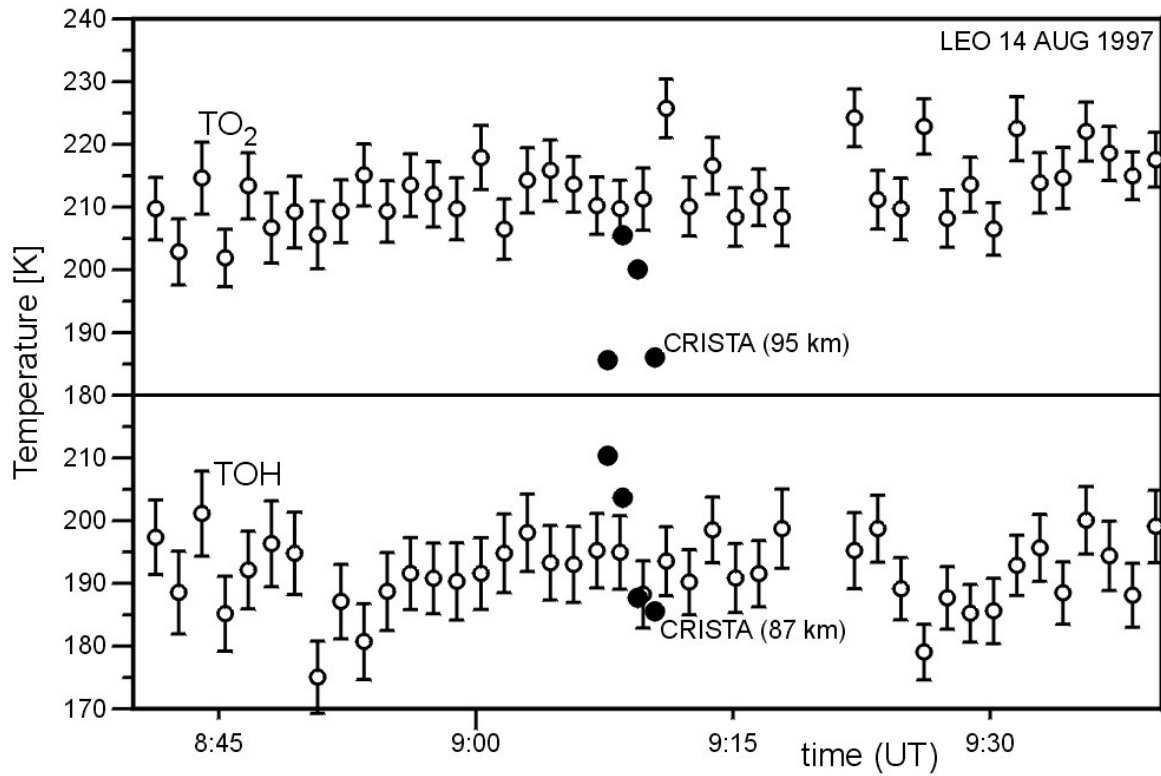


Fig. 2. Temporal variations of ground-based (open circles) and airglow-equivalent CRISTA temperatures (dots) for the same overpass as in Fig. 1. Upper (lower) panel shows O_2 (OH) rotational temperatures and CRISTA data at 95 km (87km). Error bars for airglow temperatures are derived from photon statistics. CRISTA errors (not shown) are approximately the size of the symbols.

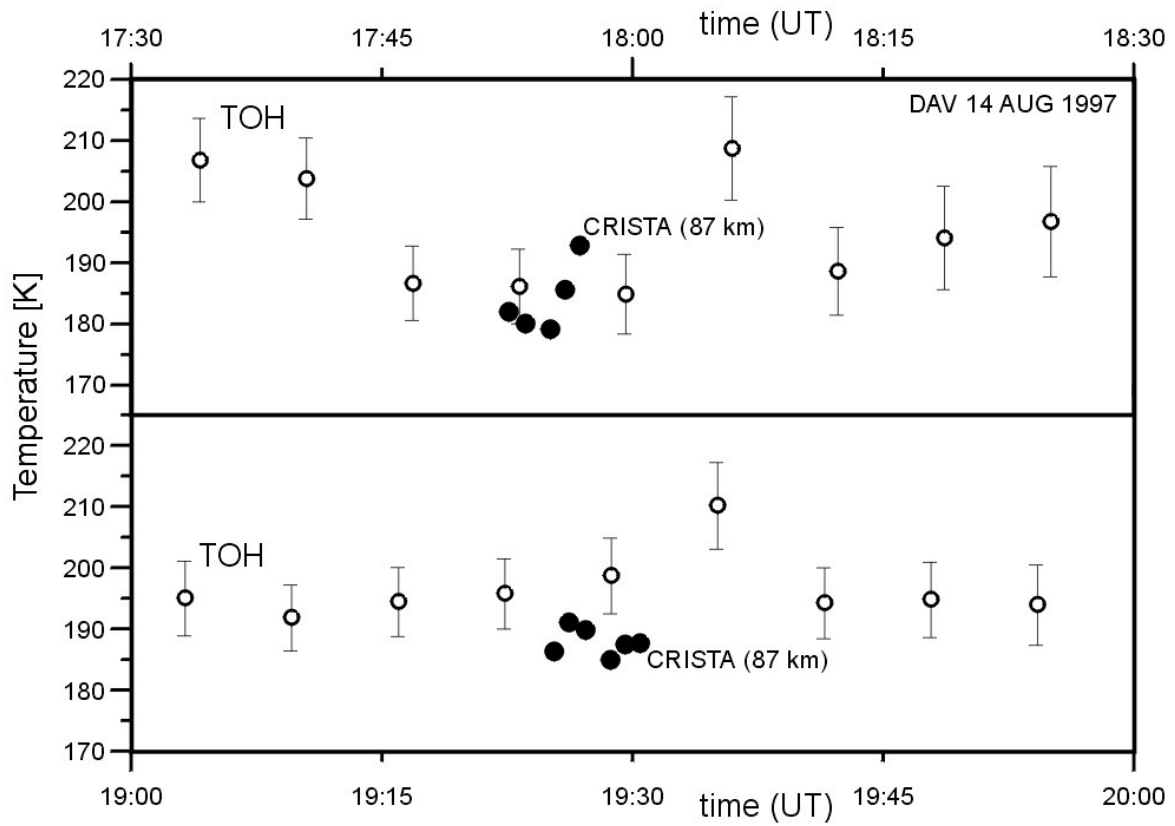


Fig. 3. Temporal variations of ground-based (open circles) and airglow-equivalent CRISTA temperatures (dots) during two consecutive overpasses at Davis (DAV). Time scale for the upper panel is shown on top. As in Fig. 2, error bars for airglow temperatures are derived from photon statistics.

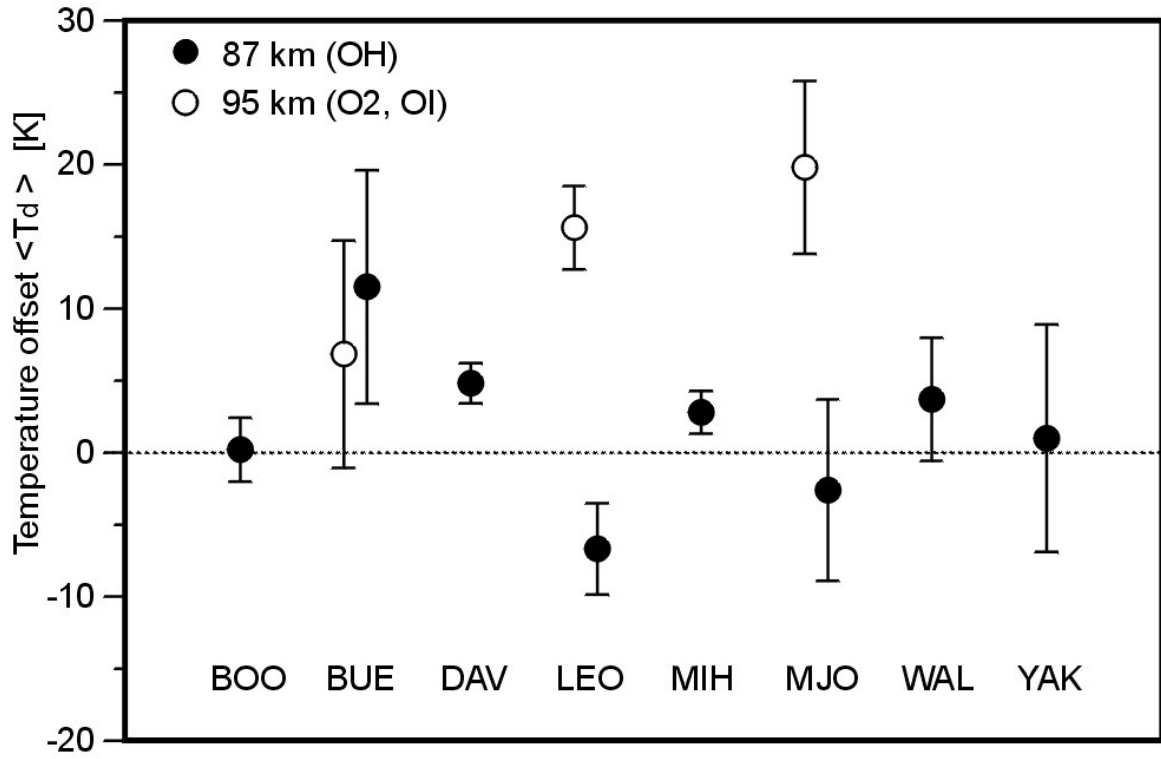


Fig. 4. Mean differences between ground-based and CRISTA temperatures for the different sites, as listed in Table 3. Dots are for OH and CRISTA temperatures at 87 km, open circles for O₂ and CRISTA at 95 km (for MJO, OI558 Doppler temperature at 96 km). Zero level is marked as dotted line to guide the eye.